Available online at www.sciencedirect.com

ScienceDirect

Ceramics International 37 (2011) 349–354

CERAMICS
INTERNATIONAL

www.elsevier.com/locate/ceramint

Effect of TiO_2 on phase evolution and microstructure of $MgAl_2O_4$ spinel in different atmospheres

R. Naghizadeh, H.R. Rezaie *, F. Golestani-Fard

Department of Metallurgical and Materials Engineering, Iran University of Science and Technology (IUST), Iran

Received 21 December 2009; received in revised form 6 July 2010; accepted 30 August 2010
Available online 29 September 2010

Abstract

The effect of TiO_2 on the formation and microstructure of magnesium aluminate spinel ($MgAl_2O_4$) at 1600 °C in air and reducing conditions were investigated. Under reducing conditions, stoichiometric $MgAl_2O_4$ spinel shifted toward alumina-rich types owing to volatilization of MgO, resulting in an increase in the porosity of fired samples. Addition of graphite to mixtures of MgO and Al_2O_3 intensified the reducing conditions and accelerated the formation of non-stoichiometric $MgAl_2O_4$. For TiO_2-containing samples on addition of $MgAl_2O_4$, magnesium aluminum titanium oxide ($Mg_xAl_{2(1-x)}Ti_{(1+x)}O_5$, $x = 0.2$ or 0.3) was detected as a minor phase. Under reducing conditions, XRD peak shifts were smaller for TiO_2-containing samples than for samples without TiO_2 owing to the formation of a solid solution of TiO_2 in $MgAl_2O_4$ and establishment of alumina-rich spinel, which have opposite effects on increasing the lattice parameter. In bauxite-containing samples, $MgAl_2O_4$ spinel, corundum, magnesium orthotitanate spinel (Mg_2TiO_4) and amorphous phases were identified. Mg_2TiO_4 spinel formed a complete solid solution with $MgAl_2O_4$ spinel but Mg_2TiO_4 remained as a distinct phase owing to the heterogeneous microstructure of bauxite-containing samples. Also dense microstructure established in air fired TiO_2 containing samples. The results are discussed with emphasis on the application and design of alumina–magnesiacarbon refractory materials, which are used in the steel industry.

Keywords: D. TiO_2; $MgAl_2O_4$; Bauxite; Alumina-rich spinel; Mg_2TiO_4

1. Introduction

Magnesium aluminate spinel is an important refractory material because of its excellent properties such as high melting point (2105 °C), low thermal expansion, high thermal spalling and corrosion resistance [1]. Dense spinel can be prepared by reaction of magnesium and aluminum compounds, generally in a two-stage firing process, with spinel formation at ~1400 °C and densification at ~1700 °C [2,3]. This approach is used because of the high volume expansion (~5%) that occurs during spinel formation that prevents densification of the product. Therefore, additives such as TiO_2, ZnO and CaF_2 were proposed for the formation and densification of magnesium aluminate spinel [1,4]. TiO_2 improved the density of spinel ceramics and had no influence on the phase constituents up to 2 wt.% [4]. A decrease in grain size and an increase in the roundness of spinel grains are the other effects of TiO_2 in spinel [4,5]. All studies were carried out in an ambient atmosphere and little information has been reported on the effect of the atmosphere. Although the effect of TiO_2 addition has been investigated, the influence of TiO_2-bearing additives such as bauxite is not really understood.

A new generation of materials called alumina–magnesia–carbon (AMC) refractory materials has become of interest for application in ladle furnaces in the steel industry. The presence of carbon in this type of material creates a reducing environment in the interior parts of linings. This can cause volatilization of Mg and variations in spinel chemistry [6]. In the present study the stability of $MgAl_2O_4$ in the presence of TiO_2 at 1600 °C in air and a reducing atmosphere is reported.

2. Experimental procedures

The raw materials were calcined alumina (Fiberona, India, >99.3% purity, $d_{50} = 2$ μm), titanium oxide (Merck, >99% purity, $d_{50} = 3$ μm), magnesium oxide (Merck, >98% purity, $d_{50} = 4$ μm) calcined bauxite (Bigglar, Iran, $d < 73$ μm) and

---

* Corresponding author. Tel.: +98 91 21025394; fax: +98 21 77240480.
E-mail address: hrezaie@iust.ac.ir (H.R. Rezaie).

0272-8842/$36.00 © 2010 Elsevier Ltd and Techna Group S.r.l. All rights reserved.
doi:10.1016/j.ceramint.2010.09.016

flake graphite (Qingda, China, >96% purity, $d < 150$ μm). Iranian calcined bauxite had the following chemical composition: Al_2O_3 64.8 wt.%, SiO_2 21.7 wt.%, TiO_2 12.15 wt.%, Fe_2O_3 1.13 wt.% and 0.54 wt.% alkali. The mineralogical configurations were corundum (major phase), mullite, tialite ($Al_2O_3 \cdot TiO_2$) and rutile. Four batch compositions were selected in such a way that they contain Al_2O_3 and MgO in a stoichiometric ratio with or without 10 wt.% graphite. TiO_2 (4 wt.%) and calcined bauxite were also used as additives. The amount of bauxite was calculated to introduce 4 wt.% TiO_2 to the batch composition with respect to stoichiometric ratio of Al_2O_3 and MgO. The sample without additives is denoted as SP and samples containing graphite, titanium oxide and bauxite as SPG, SPT and SPB, respectively. All of the batches were ball-milled in isopropyl alcohol for 4 h. The resulting slurries were dried at 110 °C and agglomerates were broken up. The batches were then mixed with 2 wt.% novalak liquid resin as binder and 0.2 wt.% hexamine as hardner, aged for 24 h and then uniaxially pressed into a cylindrical shape ($\varnothing = 50$ mm) under pressure of 150 MPa. After curing (200 °C), the samples were fired at 1600 °C at a heating rate of 5 °C min^{-1} and a soaking time of 3 h in an electric furnace in either air or a carbon bed. Samples fired under reducing conditions are denoted with the suffix E (e.g. SPE and SPTE). Crystalline phases of the samples were characterized using X-ray diffraction (XRD, Cu Kα, Philips D80). The lattice parameter a was calculated from the characteristic XRD peaks of the $MgAl_2O_4$ spinel phase using the following equation [7]:

$$a = \left(\frac{\lambda}{2}\right)\frac{(h^2 + k^2 + l^2)^{1/2}}{\sin\theta} \qquad (1)$$

where λ is the radiation wavelength, θ is Bragg's angle and ($h\ k\ l$) are the corresponding Miller indices. The microstructure of polished and coated samples was investigated under a scanning electron microscope (SEM, Cambridge S360) equipped with an energy-dispersive spectroscope. Backscattered electron imaging was also used.

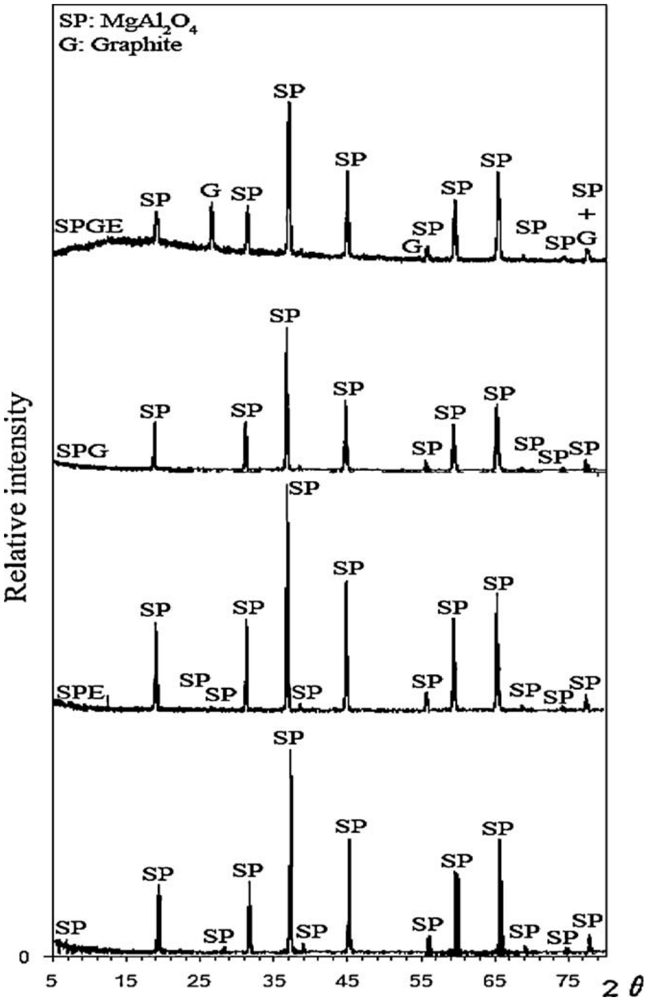

Fig. 1. XRD patterns for spinel samples with or without graphite addition after firing at 1600 °C for 3 h in air (SP and SPG) or a reducing (SPE and SPGE) atmosphere.

3. Results and discussion

XRD patterns for samples with equimolar Al_2O_3 and MgO and containing graphite after firing at 1600 °C for 3 h in air (SP and SPG) or a reducing atmosphere (SPE and SPGE) are shown in Fig. 1. The presence of $MgAl_2O_4$ spinel is evident for all samples, with no unreacted corundum or periclase phases detected. For the SPGE sample, graphite peaks were also observed.

It has been reported that the formation of magnesium aluminate spinel from its constituent oxides by diffusion of Al^{3+} and Mg^{2+} ions (Wagner mechanism) starts around 1100 °C and is complete at around 1400 °C [8,9] It depends on grain size of sample. Fig. 1 shows that at 1600 °C complete formation of spinel, with a slight shift of the XRD peaks to higher 2θ values under reducing conditions in comparison to air-fired samples. The shift in 2θ values and change in lattice parameter indicate that stoichiometric spinel changed to alumina-rich spinel [10]. Spinel easily forms a solid solution with alumina resulting in the composition $MgO \cdot nAl_2O_3$, where n varies from 1 to 7.3 at high temperature (~1990 °C) [11]. The excess Al^{3+} ions occupy tetrahedral sites, substituting for Mg^{2+} ions, leading to cation vacancies in the octahedral sites. This causes a decrease in the lattice parameter proportional to the amount of excess Al^{3+} owing to the smaller diameter of Al^{3+} compared to Mg^{2+} and formation of vacancies [11]. Lattice parameters were calculated for the SP, SPE, SPG and SPGE samples from the

Table 1
The amount of lattice parameter and its change in different samples after firing at 1600 °C.

Sample	a (Å)	$\Delta a/a$ (%)
SP	8.073	–
SPE	8.054	−0.235
SPG	8.061	–
SPGE	8.021	−0.496
SPTi	8.088	–
SPTiE	8.071	−0.210
SPTiG	8.072	–
SPTiGE	8.057	−0.185

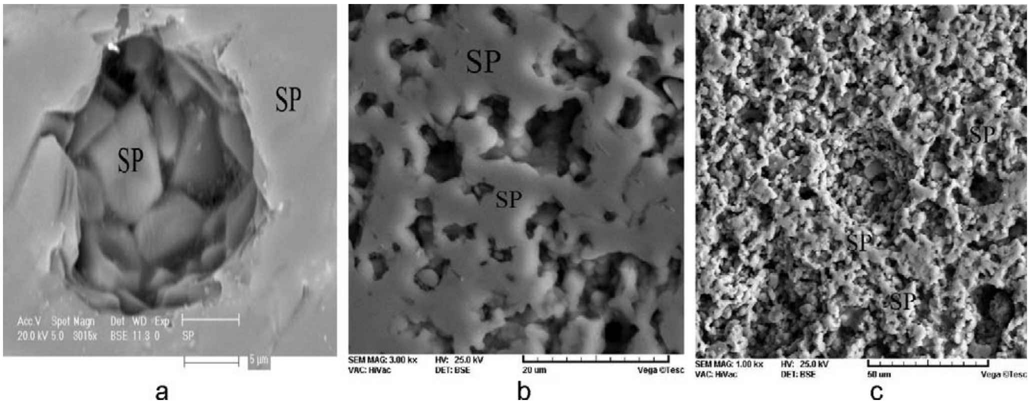

Fig. 2. SEM micrographs of the samples after firing at 1600 °C for 3 h. (a) SP, (b) SPE and (c) SPGE.

XRD peaks. The Bragg angle corresponding to the (3 1 1), (4 0 0) and (4 4 0) set of planes was used to determine values according to Eq. (1). The lattice parameter of spinel decreased in a reducing atmosphere in comparison to air-fired samples (Table 1), indicating that stoichiometric spinel was transformed to alumina-rich spinel under reducing conditions, which was particularly noticeable for sample SPGE.

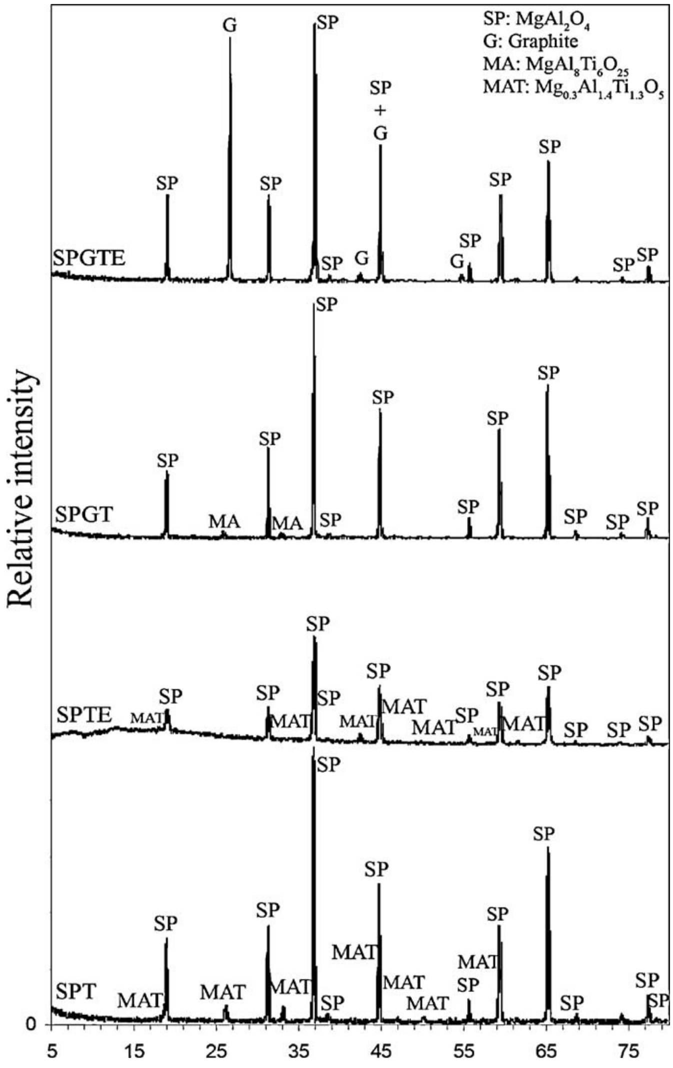

Fig. 3. XRD patterns for samples containing equimolar Al_2O_3 and MgO with TiO_2 and TiO_2 + graphite as additives fired at 1600 °C for 3 h in air (SPT and SPGT) or a reducing (SPTE and SPGTE) atmosphere.

The P_{O_2} in air is 0.21 atm and in a carbon powder bed the atmosphere contains approximately 35% CO and 65% N_2 and P_{CO} reaches almost 1 atm at >1000 °C [12,13]. The reaction at low P_{O_2} can be represented as [6]:

$$\mathrm{Mg}^{2+}(\mathrm{Al}^{3+})_2\mathrm{O}_4 \rightarrow V_{\mathrm{O}}^{\bullet\bullet} + \mathrm{Al}_{\mathrm{Mg}}^{\bullet} + V'''_{\mathrm{Al}} + \frac{1}{2}\mathrm{O}_2 + \mathrm{Mg}_{(g)} + \mathrm{Al}_{\mathrm{Al}}^{x} + 3\mathrm{O}_{\mathrm{O}}^{x} \qquad (2)$$

Escape of gaseous Mg at 1600 °C creates a porous structure in the SPE and SPGE samples, whereas no pores at inside grains were observed in the SP sample (Fig. 2). This phenomenon is particularly important in AMC refractory materials used in steel ladles because pore establishment via reduction processes may accelerate penetration of the melt and encourage chemical corrosion.

Fig. 3 shows XRD patterns for samples SPT, SPGT, SPTE and SPGTE after firing at 1600 °C in air or a reducing atmosphere. In addition to magnesium aluminate spinel,

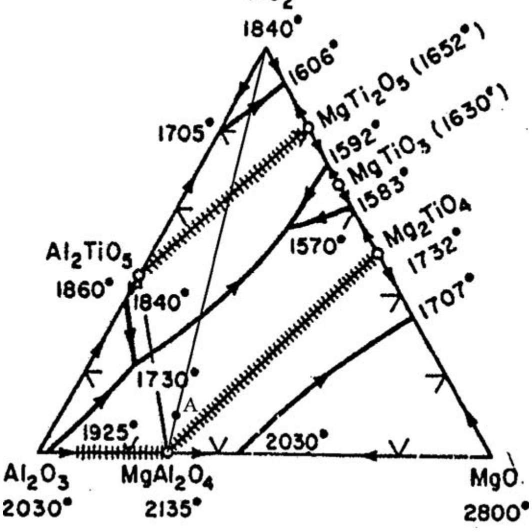

Fig. 4. MgO–Al_2O_3–TiO_2 phase diagram [14] (A: 4 wt.% TiO_2).

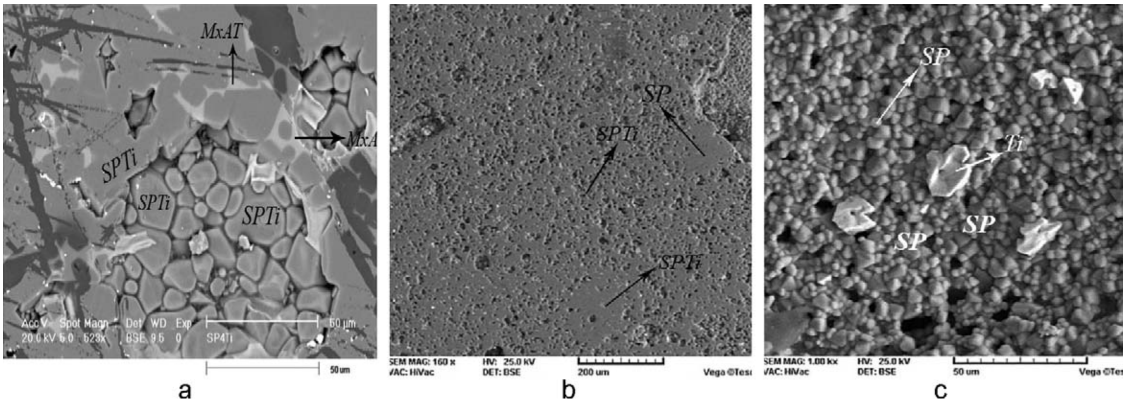

Fig. 5. SEM micrographs of samples after firing at 1600 °C for 3 h. (a) SPT, (b) SPTE and (c) SPTE. SP, spinel; SPTi, TiO_2-containing spinel; M_xAT, Mg–Al titanate; Ti, high-Ti phase.

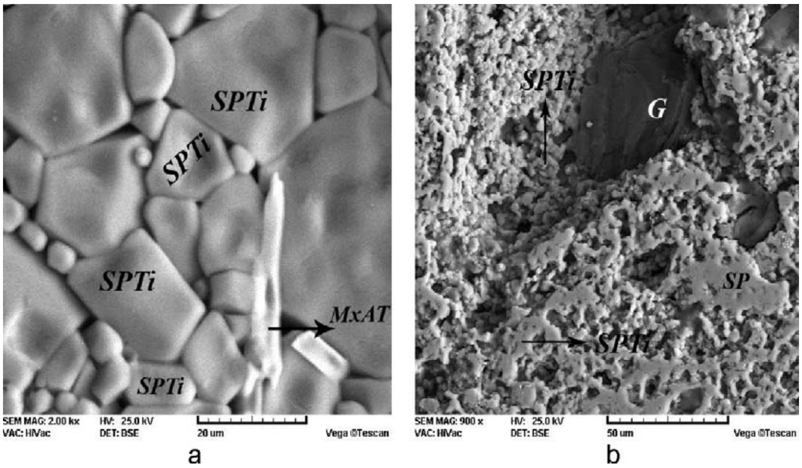

Fig. 6. SEM micrographs of samples after firing at 1600 °C for 3 h. (a) SPTG and (b) SPTGE. SP, spinel; SPTi, TiO_2-containing spinel; M_xAT, Mg–Al titanate; G, graphite.

pseudobrookite type solid solutions of Al_2TiO_5–$MgTi_2O_5$ such as $Mg_{0.3}Al_{1.4}Ti_{1.3}O_5$ ($M_{0.3}$AT) and $MgAl_8Ti_6O_{25}$ ($M_{0.2}$AT) with 33-0854, 05-0439 JCPDS card, respectively, were detected as minor phases.

According to the results in Table 1, the decrease in lattice parameter was smaller in TiO_2-containing samples than in samples without TiO_2. This phenomenon may be related to the opposite effects of TiO_2 dissolution in spinel in altering the lattice parameter and shifting stoichiometric spinel to alumina-rich spinel under reducing conditions.

When TiO_2-containing samples were fired at high temperature, a solid solution between $MgAl_2O_4$ spinel and magnesium titanate $MgTi_2O_4$ spinel formed, as shown in the $MgO–Al_2O_3–TiO_2$ phase diagram (Fig. 4) [14].

This solid solution can also be represented as [14]:

$$x\mathrm{Mg}^{2+}[\mathrm{Al}_2^{3+}]\mathrm{O}_4 + (1-x)\mathrm{Mg}^{2+}[\mathrm{Mg}^{2+}\mathrm{Ti}^{4+}]\mathrm{O}_4 \rightarrow \mathrm{Mg}^{2+}[\mathrm{Al}_{2x}^{3+}\mathrm{Mg}_{1-x}^{2+}\mathrm{Ti}_{1-x}^{4+}]\mathrm{O}_4, \quad 0 \le x \le 1 \qquad (3)$$

According to the above reaction the heterovalent substitution $2Al^{3+} \rightarrow Mg^{2+} + Ti^{4+}$ occurs in octahedral sites and changes the lattice parameter. Lattice parameters of 8.081–8.090 and 8.40–8.440 Å have been reported for $MgAl_2O_4$ and Mg_2TiO_4 samples, respectively [15]. Thus, dissolution of TiO_2 in $MgAl_2O_4$ results in an increase in lattice parameter and the corresponding XRD peaks shift to lower 2θ values. By

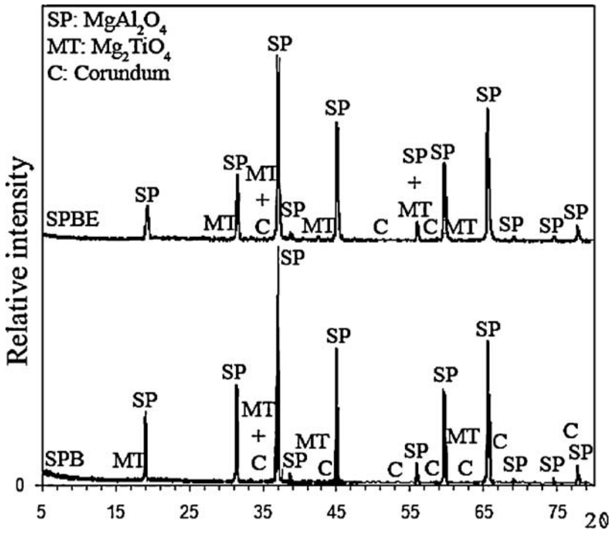

Fig. 7. XRD patterns for samples containing Al_2O_3, MgO and bauxite after firing at 1600 °C in air (SPB) or a reducing (SPBE) atmosphere.

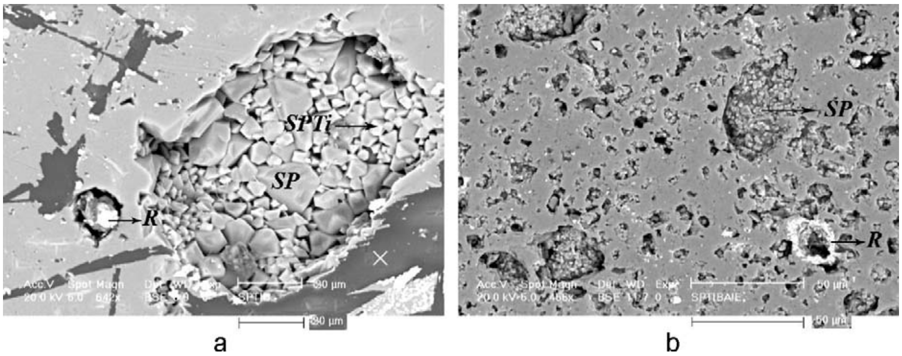

Fig. 8. SEM micrographs of samples after firing at 1600 °C for 3 h. (a) SPB and (b) SPBE. SP, spinel; R, rutile; SPTi, TiO_2-containing spinel.

contrast, reducing conditions lead to the formation of alumina-rich spinel due to reaction (2) and the XRD peaks shift to higher 2θ values. As mentioned above, magnesium aluminum titanium oxide was detected as a minor phase in SPT, SPTE and SPGT samples, but not in SPGTE (Fig. 3). This phase can be considered as a solid solution of tialite (Al_2TiO_5) and the isostructural compound $MgTi_2O_5$ [16], which has been identified as $Mg_xAl_{2(1-x)}Ti_{1+x}O_5$ (M_xAT). Pure Al_2TiO_5 tends to decompose into Al_2O_3 and TiO_2 at temperatures ranging from 750 to 1280 °C during annealing or cooling [17]. The thermal instability of Al_2TiO_5 is related to its distorted crystal structure resulting from the small ionic radius of aluminum (0.5 Å), which occupies octahedral sites [18]. On partial substitution of Al^{3+} ions by Ti^{4+} and Mg^{2+}, the thermal stability of tialite increased due to the formation of M_xAT. The presence of $M_{0.3}AT$ and $M_{0.2}AT$ in the SPT, SPTE and SPGT samples provides evidence of this phenomenon. For sample SPGTE under severe reducing conditions, due to progressive reduction of Ti^{4+} to Ti^{3+}, the stability of M_xAT decreased, resulting in elimination of this phase where is in agreement with [17].

SEM micrographs of the SPT and SPTE samples after firing at 1600 °C for 3 h are shown in Fig. 5. The SPT sample has a dense microstructure of euhedral and rounded spinel crystals containing some TiO_2 in solid solution (SPTi; Fig. 5a). The spinel grains in some areas were bounded by liquid phase sintering, as confirmed by SEM, EDS and XRD results. After firing under reducing conditions, the microstructure of sample SPTE was highly porous (Fig. 5b), probably because of magnesium volatilization according to reaction (2). In some areas, high-Ti leaf-shaped phases were enclosed by spinel crystals (Fig. 5c), probably due to reduction of residual rutile or decomposition of M_xAT phases.

Fig. 6 shows the microstructure of SPTG and SPTGE samples after firing at 1600 °C for 3 h. Fig. 6a reveals the dense microstructure of TiO_2-containing spinel crystals that bonded directly in many areas and some bright M_xAT phases present at grain boundaries. After firing under reducing conditions, non-uniform intergranular and intragranular pores, especially near graphite, severely increased in sample SPTGE.

The effect of TiO_2-containing bauxite on spinel development was also investigated. The XRD patterns for samples SPB and SPBE revealed the presence of $MgAl_2O_4$ spinel (major phase), corundum and magnesium orthotitanate spinel (Mg_2TiO_4) in these samples (Fig. 7). Owing to the formation of $MgAl_2O_4$ under reducing conditions, the corresponding XRD peaks were shifted to higher 2θ values. Mg_2TiO_4 forms a complete solid solution with $MgAl_2O_4$ at >1380 °C, but at lower temperatures this phase decomposes after several hours of annealing especially at ~1300 °C [15]. At even lower temperatures decomposition occurred for longer exposure times (up to 40 days) [15]. After firing the SPB and SPBE samples at 1600 °C, short exposure times at ~1300 °C were not sufficient for decomposition of the solid solution. Thus, owing to the presence of Mg_2TiO_4 in these samples, it seems that this phase cannot dissolve in $MgAl_2O_4$ spinel during firing. This can probably be attributed to the highly heterogeneous structure of the samples, as shown in Fig. 8a for sample SPB.

In the center of this figure, areas of $MgAl_2O_4$ spinel with (SPTi) or without TiO_2 (SP) of different size are present and different areas with a high (bright) or low TiO_2 content (gray) are evident, indicating the presence of amorphous and crystalline phases. The microstructure of sample SPBE (Fig. 8b) has a porous structure similar to that of other samples fired under reducing conditions. This specimen, similar to SPB, has different areas with highly crystalline spinel (SP) and high-TiO_2 phases (R).

4. Conclusions

The effect of high-purity rutile and TiO_2-containing bauxite on the formation and stability of $MgAl_2O_4$ spinel after firing in air or a reducing atmosphere was investigated. Firing in a reducing atmosphere shifted the XRD peaks to higher 2θ values compared to air-fired samples, indicating that stoichiometric spinel changed to alumina-rich spinel. The porosity of samples fired in a reducing environment severely increased in comparison to air-fired samples. In addition to $MgAl_2O_4$ spinel, $Mg_xAl_{2(1-x)}Ti_{1+x}O_5$ ($x = 0.2$ or 0.3) were identified as minor phases in rutile-containing samples and Mg_2TiO_4 spinel and corundum in bauxite-containing samples. The presence of graphite in the samples intensified these phenomena. After firing at air atmosphere, in TiO_2 containing samples, dense microstructure due to liquid phase sintering and formation of new phases (M_xAT) at grain boundaries were established.

References

[1] A. Ghosh, S.K. Das, J.R. Biswas, H.S. Tripathi, G. Banerjee, The effect of ZnO addition on the densification and properties of magnesium aluminate spinel, Ceram. Int. 26 (2000) 605–608.

[2] M.A. Serry, S.M. Hammad, F.M. Zawrah, Phase composition and microstructure of refractory $MgAl_2O_4$ spinel grains, Br. Ceram. Trans. 97 (6) (1998) 275–282.

[3] A.D. Mazzoni, M.A. Saniz, A. Caballero, E.F. Agliett, Formation and sintering of spinels ($MgAl_2O_4$) in reducing atmospheres, Mater. Chem. Phys. 78 (2002) 30–37.

[4] R. Sarkar, G. Bannerjee, Effect of addition of TiO_2 on reaction sintered MgO–Al_2O_3 spinels, J. Eur. Ceram. Soc. 20 (2000) 2133–2141.

[5] S. Maitra, S. Das, A. Sen, The role of TiO_2 in the densification of low cement Al_2O_3–MgO spinel castable, Ceram. Int. 33 (2007) 239–243.

[6] M.A. Saniz, A.D. Mazzoni, E.F. Aglietti, A. Caballero, Thermochemical stability of spinel ($MgO{\cdot}Al_2O_3$) under strong reducing conditions, Mater. Chem. Phys. 86 (2004) 399–408.

[7] B.D. Cullity, Elements of X-ray Diffraction, 2nd ed., Addison Wesley, Reading, MA, 1978, p. 351.

[8] R. Sarkar, A. Ghosh, S.K. Das, Reaction sintered magnesia rich magnesium aluminate spinel: effect of alumina reactivity, Ceram. Int. 29 (2003) 407–411.

[9] R. Naghizadeh, H.R. Rezaie, F. Golestani-Fard, Effect of antioxidants and atmosphere on the phase formation and microstructure of in situ MgO–Al_2O_3 spinel, Defect Diffus. Forum l5 (2008) 554–559.

[10] L. Yuanbing, L. Nan, R. Guozhi, L. Jianwei, L. Xiaohui, Effects of technical factors on $MgAl_2O_4$–TiN composites produced by aluminothermic reduction and nitridation, Mater. Des. 28 (2007) 969–972.

[11] J.S. Yong, L.L. Bin, H.N. Kang, Z. Jin, L. Youg, Investigation on lattice constants of Mg–Al Spinels, J. Mater. Sci. Lett. 19 (2000) 225–227.

[12] S. Zhang, N.J. Marriott, W.E. Lee, Thermochemistry and microstructures of MgO–C refractories containing various antioxidants, J. Eur. Ceram. Soc. 21 (2001) 1037–1047.

[13] A. Yamaguchi, Affects of oxygen and nitrogen partial pressure on stability of metal, carbide, nitride and oxide in carbon-containing refractories, Taikabutsu Overseas 7 (1) (1987) 4–13.

[14] E.M. Levin, C.R. Robbins, H.F. McMurdie, Ceramic phase diagram, 1 (714), 1985.

[15] M.A. Petrova, G.A. Mikirticheva, A.S. Novikova, V.F. Popova, Spinel solid solution in the systems $MgAl_2O_4$–$ZnAl_2O_4$ and $MgAl_2O_4$–Mg_2TiO_4, J. Mater. Res. 12 (10) (1997) 2584–2588.

[16] V. Buscaglia, F. Caracciolo, M. Leoni, P. Nanni, M. Viviani, J. Lemaitre, Synthesis sintering and expansion of $Al_{0.8}Mg_{0.6}Ti_{1.6}O_5$: a low-thermal-expansion material resistant to thermal decomposition, J. Mater. Sci. 32 (1997) 6525–6531.

[17] R. Naghizadeh, H.R. Rezaie, F. Golestani-fard, The influence of composition, cooling rate and atmosphere on the synthesis and thermal stability of aluminum titanate, Mater. Sci. Eng. B 157 (2009) 20–25.

[18] G. Tilloca, Thermal stabilization of aluminum titanate and properties of aluminum titanate solid solutions, J. Mater. Sci. 26 (1991) 2809–2814.